

Coexistence of charge density wave and antiferromagnetism in $\text{Er}_5\text{Ir}_4\text{Si}_{10}$

This article has been downloaded from IOPscience. Please scroll down to see the full text article.

2002 J. Phys.: Condens. Matter 14 5067

(<http://iopscience.iop.org/0953-8984/14/20/302>)

View [the table of contents for this issue](#), or go to the [journal homepage](#) for more

Download details:

IP Address: 171.66.16.104

The article was downloaded on 18/05/2010 at 06:41

Please note that [terms and conditions apply](#).

Coexistence of charge density wave and antiferromagnetism in $\text{Er}_5\text{Ir}_4\text{Si}_{10}$

F Galli¹, R Feyerherm², R W A Hendrikx¹, E Dudzik²,
G J Nieuwenhuys¹, S Ramakrishnan³, S D Brown⁴, S van Smaalen⁵
and J A Mydosh¹

¹ Kamerlingh Onnes Laboratory, Leiden University, NL-2300 RA Leiden, The Netherlands

² Hahn–Meitner Institute, D-14109 Berlin, Germany

³ Tata Institute of Fundamental Research, Mumbai 400 005, India

⁴ European Synchrotron Radiation Facility (XMas), F-38043 Grenoble, France

⁵ Laboratory of Crystallography, University of Bayreuth, D-95440 Bayreuth, Germany

E-mail: galli@phys.leidenuniv.nl

Received 21 March 2002

Published 9 May 2002

Online at stacks.iop.org/JPhysCM/14/5067

Abstract

$\text{Er}_5\text{Ir}_4\text{Si}_{10}$ exhibits three phase transitions upon cooling below room temperature. At $T_{\text{CDW}} = 151$ K a combined commensurate and incommensurate superstructure develops, that has been attributed to the formation of charge density waves (CDWs). At $T_{\text{LI}} = 60$ K (LI = lock-in) the superstructure becomes commensurate, and at $T_N = 2.8$ K a state with long-range antiferromagnetic order develops. In this contribution we report the results of high-intensity, high-resolution x-ray diffraction for the temperature region encompassing all four phases. We have found that above T_{CDW} the critical scattering of the commensurate superlattice reflections persists up to much higher temperatures than the critical scattering of the incommensurate satellites. It is argued that this finding substantiates the hypothesis in which the mechanism of the CDW transition involves a structural transition towards a twofold superstructure. The superlattice reflections are found to be broader in the lock-in phase than above T_{LI} . This suggests that the lock-in transition results in relatively small domains, that are responsible for the broadening of the reflections. Finally, the antiferromagnetic order is observed by resonant x-ray scattering. The commensurate superlattice reflections persist down to 1.87 K, and no effect of the magnetic transition on their positions or intensities is found. Thus the magnetic order and the CDW coexist below T_N in this compound.

1. Introduction

Charge density waves (CDWs) are collective phenomena occurring in low-dimensional conductors: they were first addressed in the 1950s by Fröhlich [1] and Peierls [2] and then

discovered experimentally later, when technologies for preparing crystals with linear chains and metallic conductivity became available [3]. The highly anisotropic topology of the Fermi surface in these systems (sometimes called *perfect nesting*) leads to a structural instability. Both the electron density of the conduction band and the atomic positions are periodically modulated along the direction of the chains, as described by a wavevector $q = 2k_F$, where k_F is the Fermi wavevector. In purely one-dimensional systems true long-range order cannot exist, and the instability is expressed through fluctuations. Most real systems are quasi-one-dimensional: this means that weak interactions between the chains are realized via

- (i) Coulomb interaction between electrons on neighbouring chains and
- (ii) one-electron inter-chain tunnelling.

This implies that at sufficiently low temperatures the system may undergo a phase transition towards a state that is characterized by a static periodic lattice distortion (PLD) and a modulation of the conduction electron density. The mean-field scenario [1] is one theoretical approach towards the description of the CDW phenomena. It neglects the fluctuations, and therefore predicts a too high transition temperature (T_{CDW}) and underestimates the experimental Δ/T_{CDW} ratios (Δ is the gap, at $T = 0$ K, opened in the Fermi surface by the CDW). In order to explain this discrepancy, a treatment is required that deals with *strong* electron–phonon coupling and/or *small* inter-chain coherence lengths. The importance of the phonons and of the three-dimensional couplings in CDW systems was addressed by McMillan [4] and Varma [5]. Studies of novel three-dimensional CDW metals, i.e. with very strong electron–phonon coupling, would test such theories.

CDWs, being manifestations of the collective behaviour of the electrons and the phonons simultaneously, are often interesting when they appear together with other phenomena such as superconductivity and magnetism. The ternary rare-earth (RE) intermetallic compounds $\text{RE}_5\text{Ir}_4\text{Si}_{10}$ have been studied recently because of their multiple ground states, like CDWs [6–8], magnetism [6, 9, 10] and superconductivity [7]. Here, the REs play a unique role because of the 4f electrons, which determine their magnetic properties. Due to the very small or negligible overlap between f orbitals, the magnetic moments are well localized, and therefore the mechanism involved in the magnetic interactions is indirect exchange via the itinerant conduction electrons [11]. The Néel temperature (T_N) predicted in this picture is proportional to the conduction electron density at the Fermi level [12]. The same conduction electrons are responsible for the CDW instability, and $\text{Er}_5\text{Ir}_4\text{Si}_{10}$ offers the unique possibility of studying the interplay of *strongly coupled* CDWs and *local moment* magnetism.

Previous studies [8] have shown that a first transition at $T = 155$ K involves the development of a combined commensurate ($q = (0, 0, 1/2)$) and incommensurate ($q = (0, 0, 1/4 \pm \delta)$, where δ is the incommensurability) superlattice. This behaviour was explained within the framework of two possible scenarios [8]: the first one ('scenario I') treating the commensurate modulation as a structural transformation which drives the one-dimensional incommensurate CDW, the second one ('scenario II') describing the commensurate CDW as a result of the interaction of two independent incommensurate waves. Upon cooling below $T_{\text{LI}} = 55$ K, the incommensurate CDW locks in, whereby the incommensurability δ drops sharply to zero. At even lower temperature (2.8 K), the intermetallic compound becomes antiferromagnetic, with the ordered Er^{3+} moments aligned along the *c*-axis and with a magnetic unit cell which is doubled in the basal plane [10]. The possible interplay and/or coexistence of the CDW phenomena with the long-range antiferromagnetism was addressed but not proven.

In this paper we report detailed high-resolution and high-intensity x-ray diffraction studies on a high-quality single crystal of $\text{Er}_5\text{Ir}_4\text{Si}_{10}$ in the temperature range 1.8–300 K. Our results lead to an increased understanding of the phase transitions in this compound. They can be summarized as follows. The observation of critical scattering due to fluctuations around

the high-temperature transition strongly suggests that the mechanism of this transition is a commensurate structural transformation followed by the development of an incommensurate CDW. A sudden broadening of the superlattice lines on cooling below T_{LI} indicates the formation of domains. Finally, we have observed the coexistence of long-range magnetic order and the CDW superlattice below T_N .

2. Experimental details and results

Single crystals of $\text{Er}_5\text{Ir}_4\text{Si}_{10}$ were grown with the tri-arc Czochralski technique as described elsewhere [8]. The crystals were analysed with electron-probe microanalysis and the secondary phases found to be $<1\%$. Powder and single-crystal x-ray diffraction at room temperature showed that the samples have tetragonal structure (space group $P4/mbm$) and lattice parameters $a = b = 12.543(1) \text{ \AA}$ and $c = 4.203(1) \text{ \AA}$ (see figure 1 of [8]). For the synchrotron experiment, we cut a parallelepiped-shaped sample of size $1.9 \times 2.0 \times 3.0 \text{ mm}^3$, with one face being the (110) plane. The experiment was carried out at the European Synchrotron Radiation Facility (ESRF), beamline BM28 (XMas), in Grenoble, France [13]. The sample was mounted inside a small closed-cycle cryostat (base temperature 1.7 K) on a Huber goniometer, and the experiment performed in reflection geometry, the (110) plane being the scattering surface. A monochromatic focused beam of energy $E = 8.361 \text{ keV}$ (wavelength $\lambda = 1.483 \text{ \AA}$) was used.

In a first experiment we studied the temperature dependence of the superstructure between 5 and 300 K. Upon cooling below 153 K, a number of superlattice reflections were found. Figure 1 shows the set of superlattice reflections and a crystallographic main line, (4, 4, 1), at 150 K, from scans along (4, 4, l) with $0 < l < 1.05$. The profiles could be described by Lorentzian functions. Different attenuation factors were used, to avoid detector saturation. The intensities are normalized to the average beam current of the synchrotron during each measurement. The incommensurability δ is approximately the same for the two incommensurate reflections, as shown in figure 1, and is temperature dependent (see figure 5 in [8]). Figure 2 shows the temperature dependence of the integrated intensities of the reflections obtained from ω -scans centred at the reflection positions. The measurement was performed at a series of temperatures, on warming from 140 to 165 K. The temperature dependence of the line widths obtained from the ω -scans is presented in figure 3. Below⁶ $T_{\text{CDW}} = 151 \text{ K}$ all reflections display the same width. Above T_{CDW} , the commensurate superlattice peak is broader than the incommensurate ones. At the transition temperature the widths attain their final constant values, and they remain so down to temperatures well below T_{CDW} .

Below $T_{\text{LI}} = 60 \text{ K}$, the incommensurate CDW locks in, thus becoming commensurate. This is seen in the l -scans, whereby the incommensurability δ sharply drops to zero, and the two incommensurate peaks merge, leading to commensurate lines at (4, 4, 1/4) and (4, 4, 3/4) (not shown). It is found that this transition is accompanied by a sudden increase of the width of the superlattice reflections, while the main reflections (e.g. the (4, 4, 1)) are not affected, as shown in figure 4. The temperature dependence of the intensities around the lock-in transition temperature T_{LI} is hysteretic (not shown). This agrees with previous electrical resistivity measurements [8] and is attributed to the *first-order* character of the lock-in transition in this system.

In a second experiment, the x-ray scattering was measured below 5 K. At $T_N = 2.8 \text{ K}$, $\text{Er}_5\text{Ir}_4\text{Si}_{10}$ becomes antiferromagnetically ordered. The magnetic structure has already been

⁶ In the experiment reported in [8] it was found that $T_{\text{CDW}} = 155 \text{ K}$, due to the fact that a different crystal and cryostat were used.

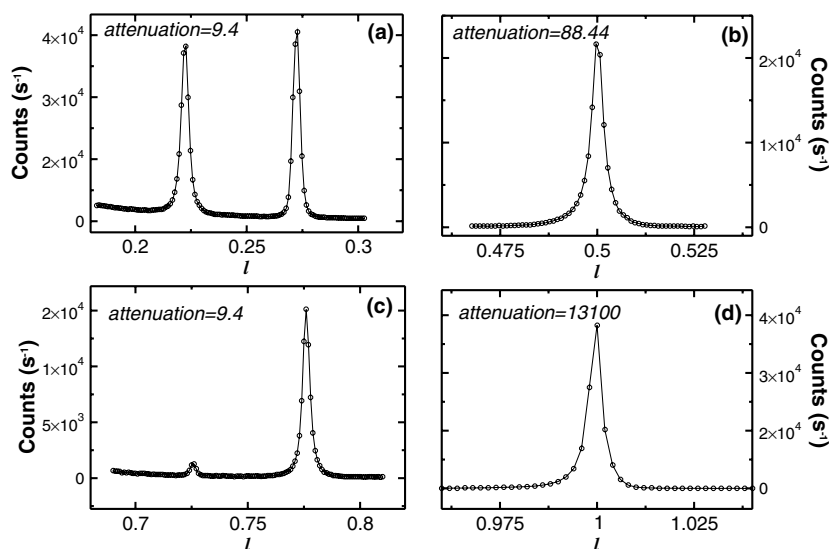


Figure 1. The $(4, 4, 1/4 \pm \delta)$ (a), $(4, 4, 1/2)$ (b) and $(4, 4, 3/4 \pm \delta)$ (c) superlattice reflections, at 150 K. Here δ (incommensurability) is $|x_c - 1/4| \approx |x_c - 3/4| \approx 0.023(5)$, where x_c is the centre of the Lorentzian. The main reflection $(4, 4, 1)$ (d) is also shown for comparison. The attenuation factors used are shown. The continuous curve is the fitted Lorentzian profile.

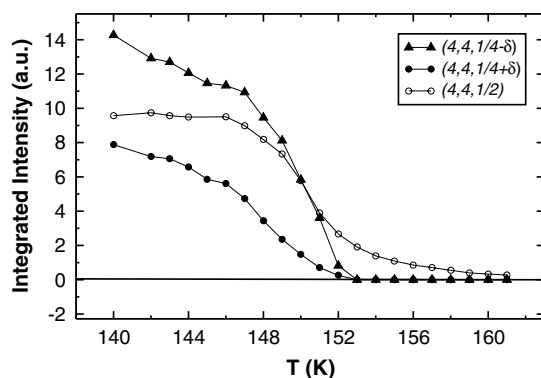


Figure 2. Integrated intensity of the superlattice reflections versus temperature, on warming from 140 up to 165 K. The continuous curves are a guide to the eye.

investigated via neutron diffraction techniques [10]. A number of magnetic Bragg reflections of the type $(h/2, k/2, 0)$ were found, and a magnetic structure model was developed, involving a unit cell doubled in the basal plane and the Er^{3+} moments being aligned antiferromagnetically along the c -axis. The commensurate CDW superlattice reflections at $(h, k, l \pm 1/4)$ or at $(h, k, l + 1/2)$ could not be seen in the neutron scattering due to lack of high intensity, leaving the question about the interactions between the CDW and the magnetism unanswered.

In the present experiment the magnetic transition was followed by resonant magnetic x-ray scattering at the L edges of Er (8.361 keV) and Ir (11.211 keV). Upon cooling below 2.8 K, two dominant magnetic reflections, $(3/2, 3/2, 0)$ and $(5/2, 5/2, 0)$, were observed for $E = 8.361$ keV. No resonance enhancement could be seen either for a photon energy off resonance or at the L edge of Ir, indicating that the latter element does not contribute to

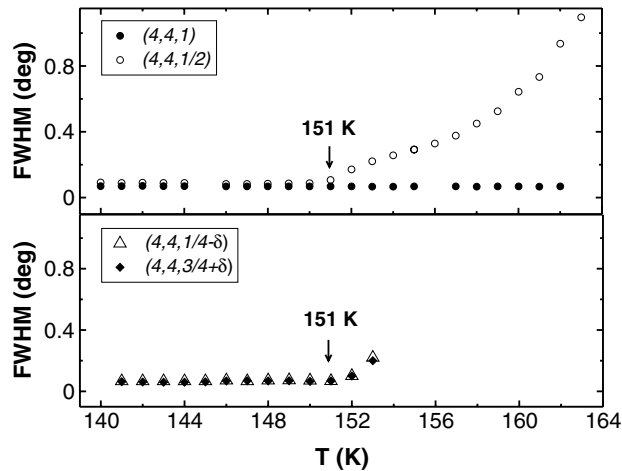


Figure 3. The line width (FWHM) from ω -scans versus temperature, for $140 < T < 163$ K. The transition temperature is indicated. The incommensurate reflections (lower plot) disappear above 153 K (see also figure 2).

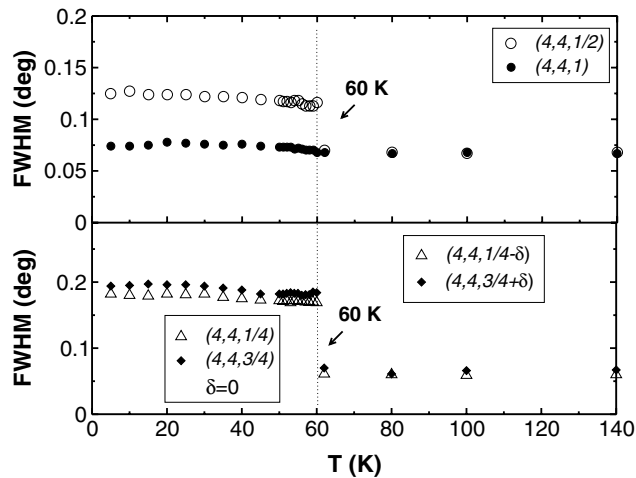


Figure 4. The line width (FWHM) from ω -scans versus temperature, for $5 < T < 140$ K. The lock-in transition temperature is indicated. In the commensurate state (left-hand side of the dotted line, $\delta = 0$) the line width of the CDWs shows a steplike increase.

the magnetism in this system. Figure 5 shows the temperature dependence of the measured magnetic lines. The integrated intensities are normalized to the intensity at the lower temperature, 1.87 K. The lower plot also displays the square root of the intensity for the $(3/2, 3/2, 0)$ line as observed from neutron diffraction experiments [10]. In figure 6, the intensities of the CDW superlattice reflections are shown for temperatures lower than 3.3 K. No effect of the magnetic transition was found, either on the integrated intensities, or on the width of the peaks, or on their position. This observation proves that there is no apparent coupling between the CDW and the magnetic order.

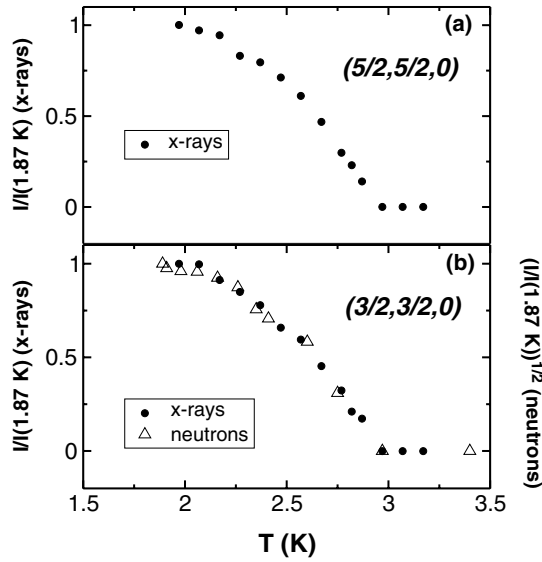


Figure 5. (a) Temperature dependence of the integrated intensity of resonant magnetic Bragg reflection $(5/2, 5/2, 0)$. (b) Temperature dependence of the intensity of resonant magnetic Bragg reflection $(3/2, 3/2, 0)$, compared with the temperature dependence of the square root of the intensity of the same reflection, but from previous neutron diffraction data [10].

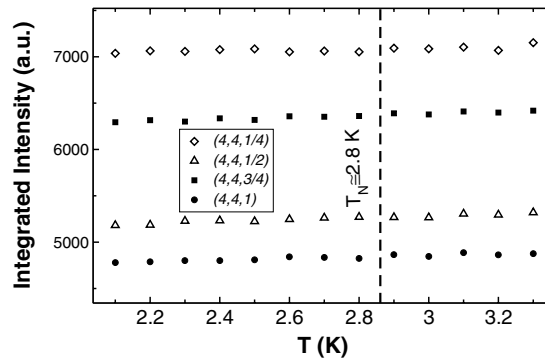


Figure 6. Temperature dependence of the integrated intensities of the superlattice reflections $(4, 4, 1/2)$, $(4, 4, 1/4)$ and $(4, 4, 3/4)$ and of the main line $(4, 4, 1)$ upon cooling below $T_N = 2.8$ K.

3. Discussion

Figures 2 and 3 give new experimental information on the character of the transition at T_{CDW} . As stated above, we defined T_{CDW} as the temperature at which the line-width of the superlattice reflections becomes constant, that is, where the long-range order has fully developed. In figure 3, the line-width reaches the lowest and constant value at the same temperature (151 K) for all the $(4, 4, 1/4 - \delta)$, $(4, 4, 3/4 + \delta)$ and $(4, 4, 1/2)$ reflections. Accordingly, we can conclude that the ordering temperature is the same for both the commensurate and incommensurate superstructures, namely 151 K, even if the number of experimental points in the critical region (which could be small) is not enough to discriminate between this case or the possibility of having two different, but very close, critical temperatures. We observe the presence of critical

scattering before the actual phase transition takes place ($151 < T < 162$ K), for the commensurate reflection. The fact that the $(4, 4, 1/2)$ reflection is broader above 151 K suggests that the fluctuations of the order parameter are much larger for this commensurate transformation than for the incommensurate CDW. The intensity of the incommensurate lines vanishes above 153 K, as shown in figure 2, while pre-transitional effects are clearly seen for the commensurate line, which disappears at a higher temperature (162 K). These results support the mechanism for the phase transition in which at 151 K a purely *structural* transformation to a state with a unit cell doubled along the c -axis occurs ('scenario I'). The modified band structure of this doubled cell then enhances nesting and the development of the incommensurate CDW. The latter can be described by the single modulation wavevector $\mathbf{q} = (0, 0, 1/2 - 2\delta)$ in the new unit cell.

The conjecture that the commensurate periodic modulation could be of a different origin than electronic is also corroborated by the evidence of a very sharp anomaly at T_{CDW} in the specific heat [8]. The large ratio $\Delta C/T_{\text{CDW}}$ ($0.6 \text{ J mol}^{-1} \text{ K}^{-2}$) cannot be fully accounted for by strongly coupled theories of CDWs [4, 5]. Preliminary band structure calculations suggest a unique nesting condition in the Fermi surface along the c -axis [14]. The idea of a one-dimensional incommensurate CDW is also supported by the fact that all incommensurate reflections are described by a single incommensurability δ and that they have similar temperature dependences [8]. Nevertheless, a full structural refinement below T_{CDW} is a necessary prerequisite for a conclusive statement on the nature of this unusual transition.

The alternative scenario ('scenario II'), in which the commensurate modulation is treated as a commensurate CDW resultant of two incommensurate CDWs, i.e. with two *independent* nesting vectors, cannot explain the presence of fluctuations above 153 K exclusively for the $(4, 4, 1/2)$ line (figures 2 and 3).

Below T_{CDW} the line-width of the commensurate reflection is $\approx 0.02^\circ$ larger than that of the incommensurate reflections and of the main line (figure 3), suggesting that the correlation length of the commensurate order is smaller. In the pre-transitional region, $151 < T < 162$ K, as well as in the ordered state, the profile is fitted with a single Lorentzian shape (figure 1): in other words there is no evidence for a second length scale of the critical fluctuations [15].

The lock-in transition at $T_{\text{LI}} = 60$ K was found to be accompanied by a sudden increase of the width of the reflections from 0.07 (in the incommensurate state) to 0.19° (in the commensurate state) for the incommensurate line, and from 0.09° to 0.12° for the commensurate one (figure 4). This indicates that the correlation length is reduced in the commensurate state. It can be tentatively explained within a *first-order* type of transition, where 'domains' can form. From the width of the lines in the l -scans, we estimated a domain size of few micrometres.

For temperatures lower than $T_N = 2.8$ K, we established that CDWs and long-range antiferromagnetism coexist. In figure 5, lower plot, the square root of the intensity for the $(3/2, 3/2, 0)$ magnetic line is shown from previous neutron diffraction experiments [10]. This can be directly related to the temperature dependence and the magnitude of the magnetization of the specimen. In resonant magnetic x-ray scattering there is no straightforward relation between the size of the moments and the individual intensity of the Bragg peaks of the magnetic diffractogram [16], which makes the analysis more elaborate. Nevertheless, in this case the intensity grows in a similar fashion as the magnetic moment, as extracted from neutron data. Figure 6 illustrates that there is no apparent direct coupling between the order parameters of the CDWs and the antiferromagnetism. In this sense, the two collective phenomena coexist, without any large direct interplay, which should be visible if any change could have been seen in the temperature dependence of the superlattice lines at $T_N = 2.8$ K. On the other hand, the magnetic ordering temperature should be affected by changes of the density of conduction electrons, as expected in RE intermetallic compounds in which the RKKY magnetic interaction

between local moments is supported by these spin-polarized electrons. A reduction of the density of states (DOS) at E_F is expected when a CDW occurs, due to partial gapping in the Fermi surface [17]. In $\text{Er}_5\text{Ir}_4\text{Si}_{10}$ the magnetic ordering develops at lower temperature than in isostructural compounds [18] which do not show CDWs. Alternatively, crystal electric field (CEF) effects can also introduce deviations from the de Gennes scaling rule of T_N [12]. Hence the knowledge of the DOS and of the CEF in this system, together with the size of the gap in the CDW state, is required to explain T_N .

4. Conclusions

In conclusion, our low-temperature x-ray diffraction investigation on $\text{Er}_5\text{Ir}_4\text{Si}_{10}$ demonstrates that this system is a unique example of unusually strongly coupled CDW. We suggest that a structural instability towards a transition to a state with a doubled c -axis occurs at 151 K, and this causes the one-dimensional incommensurate CDW to form. The experimental findings discussed in this work, together with the large anomaly measured in the specific heat at T_{CDW} , reinforce our first scenario versus the second one of a two-dimensional incommensurate CDW. Further progress in the determination of the band structure and the structural refinement below T_{CDW} are required for a full understanding of this unusual phase transition. This work also establishes the coexistence of the CDW and local moment antiferromagnetism in $\text{Er}_5\text{Ir}_4\text{Si}_{10}$. The development of the antiferromagnetism does not affect the CDW order parameter directly, so there is no evident coupling between the two collective phenomena. A possible effect of the CDW on the magnetism could result in a weaker magnetic interaction due to the reduction of the conduction electron DOS, and therefore a low T_N .

Acknowledgments

We gratefully acknowledge M Mostovoy (Groningen University) for useful discussions and P Thompson (ESRF) for assistance with the synchrotron radiation experiment. Part of this research is supported by the Dutch Foundation (FOM), the German Science Foundation (DFG) and the European Synchrotron Radiation Facility (ESRF). Beamtime at beamline BM28 of ESRF was awarded under general user proposal number HE-1194.

References

- [1] Fröhlich H 1954 *Proc. R. Soc. A* **223** 296
- [2] Peierls R E 1955 *Quantum Theory of Solids* (New York: Oxford University Press)
- [3] Grüner G 1994 *Density Waves in Solids* (Reading, MA: Addison-Wesley) ch 2
- [4] McMillan W L 1977 *Phys. Rev. B* **16** 643
- [5] Varma C M and Simons A L 1983 *Phys. Rev. Lett.* **51** 138
- [6] Shelton R N, Hausermann-Berg L S, Klavins P, Yang H D, Anderson M S and Swenson C A 1986 *Phys. Rev. B* **34** 4590
- [7] Becker B, Patil N G, Ramakrishnan S, Menovsky A A, Nieuwenhuys G J, Mydosh J A, Kohgi M and Iwasa K 1999 *Phys. Rev. B* **59** 7266
- [8] Galli F, Ramakrishnan S, Taniguchi T, Nieuwenhuys G J, Mydosh J A, Geupel S, Lüdecke J and van Smaalen S 2000 *Phys. Rev. Lett.* **85** 158
- [9] Ghosh K, Ramakrishnan S and Chandra G 1993 *Phys. Rev. B* **48** 4152
- [10] Galli F, Feyerherm R, Hendriks R W A, Ramakrishnan S, Nieuwenhuys G J and Mydosh J A 2000 *Phys. Rev. B* **62** 13 840
- [11] Ruderman M A and Kittel C 1954 *Phys. Rev.* **96** 99
Kasuya K 1956 *Prog. Theor. Phys., Kyoto* **16** 45
Yoshida K 1957 *Phys. Rev.* **106** 893

-
- [12] de Gennes P G 1962 *J. Phys. Radium* **23** 510
 - [13] Brown S D *et al* 2001 *J. Synchrotron Rad.* **8** 1172
 - [14] Chioncelu L and Lichtenstein A I 2001 private communications
 - [15] Altarelli M, Núñez-Regueiro M D and Papoular M 1995 *Phys. Rev. Lett.* **74** 3840
 - [16] Vettier C 1994 *J. Magn. Magn. Mater.* **129** 59
 - [17] Galli F, Nieuwenhuys G J, MacLaughlin D E, Heffner R H, Amato A, Bernal O O and Mydosh J A 2002 *Physica B* at press
 - [18] Galli F, in preparation